Biomedicine & Pharmacotherapy 191 (2025) 118490

Contents lists available at ScienceDirect

Biomedicine & Pharmacotherapy

journal homepage: www.elsevier.com/locate/biopha

Trastuzumab cardiotoxicity and drug cardioprotection in healthy and cardiac dysfunction mouse models

Serena L'Abbate [a,b], Matilde Masini [c], Giuseppina Nicolini [a], Sabrina Marchetti [a], Francesca Forini [a], Iacopo Fabiani [d], Giuseppe Vergaro [b,d], Vincenzo De Tata [c], Michele Emdin [b,d], Claudia Kusmic [a,*,1]

[a] CNR, Institute of Clinical Physiology, Pisa, Italy
[b] Health Science Interdisciplinary Center, Scuola Superiore Sant'Anna, Pisa, Italy
[c] Translational Research and New Technologies in Medicine and Surgery, University of Pisa, Italy
[d] Division of Cardiovascular Medicine, Fondazione Monasterio, Pisa, Italy

ARTICLE INFO

Keywords:
Left ventricular systolic dysfunction
Mitochondrial homeostasis
Anti-cancer therapy
Captopril
Bisoprolol
Mouse model

ABSTRACT

Pre-existing cardiovascular disease is a recognised risk factor for cardiotoxicity in HER2-targeted therapies such as trastuzumab (TRZ), but few studies have addressed the impact of TRZ and the effects of cardioprotective drugs in pre-existing cardiac issues. This study examines the impact of TRZ-induced cardiotoxicity in pre-existing cardiac conditions and the effects of captopril and bisoprolol in mouse models with varying degrees of cardiac impairment. Adult mice models with and without baseline cardiac dysfunction– healthy mice (WT), transgenic mice with cardiac hyperaldosteronism (AS) and mice with cardiac dysfunction (AS+ISO)– were randomised to receive placebo, TRZ alone (6 mg/kg/week for 4 weeks), or TRZ administered concomitantly with a cardioprotective therapy based on captopril (ACEi, 20 mg/kg) and bisoprolol (BB, 5 mg/kg) (TRZ+ACEi/BB). Cardiac function was assessed one week after the final injection of TRZ, followed by myocardial tissue histopathological and ultrastructural assessments, and expression of genes associated with cardiomyocyte survival and mitochondrial homeostasis. TRZ reduced systolic function by approximately 10 % in each of the 3 populations studied, causing cellular and mitochondrial damage, regardless of pre-existing cardiac issues. The most severe effects were observed in mice with prior cardiac impairment linked to increased baseline frailty. Cardioprotective therapy improved LV systolic function in all groups to a similar degree. It also reversed the cellular and mitochondrial adverse changes, as well as the altered transcriptional signature caused by TRZ. Our findings demonstrate that the combined ACEi/BB therapy may prevent cardiac TRZ-related toxicity in mouse models with and without baseline cardiac dysfunction.

1. Introduction

Cardiac toxicity from cancer therapies increases the risk of adverse cardiovascular (CV) events in cancer patients, posing significant challenges for cancer care. The current knowledge of cardiotoxicity has continued to evolve, and so has the awareness of different susceptibility to cancer therapies across the entire spectrum of patients. As the number of people currently living with chronic diseases is increasing [1], the chance of developing cancer also increases for patients with pre-existing CV risk factors or overt CV disease [2]. However, the safety of oncological treatments in these populations is still unexplored. As such, the impact of cardiotoxic cancer therapies in the high-risk setting is one of the leading challenges in the field of cardio-oncology [3]. Pre-existing CV disease is a recognised risk factor for future cardiotoxicity in many

List of abbreviations: ACEi, angiotensin-converting enzyme inhibitor; Bax, Bcl-2-associated X; BB, beta blocker; Bcl-2, B-cell lymphoma/leukemia 2; CSA, cross-sectional area; CV, cardiovascular; Drp-1, dynamin-related protein 1; EF, ejection fraction; Fis-1, fission protein 1; HER2, human epidermal growth factor receptor 2; LV, left ventricle/ventricular; Mfn-2, Mitofusin 2; Opa-1, optic atrophy 1; Pgc-1α, proliferator-activated receptor gamma coactivator 1–alpha; ROS, reactive oxygen species; SOD2, superoxide dismutase 2; TRZ, trastuzumab.

* Correspondence to: CNR, Institute of Clinical Physiology, Via Moruzzi 1, Pisa 56124, Italy.
E-mail address: claudia.kusmic@cnr.it (C. Kusmic).
[1] ORCID: 0000–0002-8064–8311

https://doi.org/10.1016/j.biopha.2025.118490
Received 10 July 2025; Received in revised form 20 August 2025; Accepted 23 August 2025
Available online 28 August 2025

cancer therapies, including HER2-targeted therapies such as trastuzumab (TRZ) [4]. TRZ, a humanised monoclonal antibody, was the first FDA-approved drug against HER2. In the heart, the role of HER2 is strictly related to one of the known ligands of HER receptors, the signalling protein neuregulin-1, and the downstream signalling pathways that converge on cardiomyocyte integrity, survival, and function [5].

In addition to its role in heart development [6], HER2 mediates protective responses against cardiac injury in the adult heart, as shown by the evidence that conditional ErbB2 mutant mice develop hypertrophy, ventricular dilatation, and impaired contractile function [7,8]. The relevance of the pharmacological inhibition of HER2 on cardiac homeostasis has so far been confirmed by several studies exploring the effects of TRZ in experimental models of cardiotoxicity. I*n vivo* studies confirmed systolic dysfunction as the primary manifestation of TRZ-induced cardiotoxicity [9–14], accompanied by subclinical myocardial cell injury [10,14,15]. Still, the pathophysiological events that contribute to cardiac toxicities are yet to be defined, hence precluding therapeutic strategies that may hold relevance against TRZ-induced cardiotoxicity. Although neurohormonal antagonists such as beta-blockers (BB) and angiotensin-converting enzyme inhibitors (ACEi) are currently recommended [16,17], investigations are still needed into the implications of such cardioprotective strategies after exposure to TRZ as a single agent, when it is not preceded by prior anthracycline-based therapy. To date, very few studies have focused on the safety of TRZ in patients with pre-existing cardiac disease, who are often underrepresented in oncological clinical trials. Among these, the SAFE-Heart (Prospective evaluation of the cardiac safety of HER2-targeted therapies in patients with HER2-positive breast cancer and compromised heart function) trial and the SCHOLAR (Safety of Continuing Chemotherapy in Overt Left Ventricular Dysfunction Using Antibodies to Human Epidermal Growth Factor Receptor-2) trial recently suggested that continuing TRZ may be feasible in patients with cardiac dysfunction (LVEF 40–49 %) [18] or despite mild cardiotoxicity (LVEF 40 %-54 %, or LVEF $\geq$ 54 % and an absolute fall in LVEF $\geq$ 15 % from baseline) [19], supporting the utmost importance of cardio-oncology referral to ensure the completion of planned oncological treatments uninterruptedly. Despite this clinical evidence, further studies are needed to identify the mechanistic components of TRZ-related myocardial injury and cardioprotection in high-risk settings. Among the possible approaches, modelling TRZ-induced cardiotoxicity in animal models with pre-existing cardiac dysfunction has not been tested to date [20].

Here, we investigated the role of pre-existing cardiac dysfunction in TRZ-induced cardiotoxicity and the cardioprotective efficacy of prophylactic ACEi (captopril) and BB (bisoprolol) administration, using mouse models that recapitulate different baseline risk profiles. Cardioprotection strategies with mineralocorticoid receptor antagonists and with sacubitril/valsartan have been successfully tested in a murine model of cardiac-specific hyperaldosteronism (AS mice) that received subcutaneous isoproterenol injections to induce LV systolic dysfunction [21,22].

2. Materials and methods

The Supplemental Material provides details on the procedures and statistical analyses mentioned in this document. All studies received approval from CBS Animal Care and the Italian Ministry of Health (N. 328/2021-PR), in accordance with Italian Law (D.Lgs. 26/2014), the EU Directive 2010/63/EU, and the Guide for the Care and Use of Laboratory Animals.

2.1. Animals and study design

Adult transgenic mice with cardiac-specific overexpression of the aldosterone synthase gene (AS mice) on an FVB background, along with adult wild-type FVB mice (WT mice) of both sexes, were utilised. AS mice exhibit a two-fold increase in intra-myocardial concentration of aldosterone compared to WT mice, thereby reproducing the condition of cardiac hyperaldosteronism [23]. Furthermore, this mouse model has previously been shown to develop left ventricular (LV) dysfunction when treated acutely with high doses of the β-agonist isoproterenol (ISO) [21]. To simulate progressive cardiac dysfunction, some AS mice in the present study received an acute challenge with high doses (300 mg/kg of body weight) of the β-agonist isoproterenol [22], administered twice daily for two consecutive days (AS+ISO mice).

Colonies have been locally bred from four founding female FVB mice, purchased by Envigo s.r.l (Udine, Italy), and two founding male heterozygous transgenic AS mice, provided by the Institut National de la Santé et de la Recherche Médicale U942 and Université Paris-Diderot. Further details on mouse strains and colony breeding are provided in the Supplemental Material.

Mice were enrolled in the protocol at 10–12 weeks of age. They were assessed at T0, which occurred at 12–14 weeks of age, and completed the protocol at T1, at 16–18 weeks of age. A schematic representation of the study is illustrated in Fig. 1.

Two weeks after an initial ISO injection in AS mice (T0), cardiac function was evaluated using high-frequency ultrasound imaging and surface ECG recordings. At this point, mice from all groups (WT, AS, and AS+ISO, n = 11 for each) were sacrificed to characterise the phenotypes. Remaining mice were randomly assigned to treatments: saline (WT+PBO, n = 7; AS+PBO, n = 5; AS+ISO+PBO, n = 8), trastuzumab (TRZ) (WT+TRZ, n = 9; AS+TRZ, n = 6; AS+ISO+TRZ, n = 9), or trastuzumab combined with cardioprotective therapy (WT+TRZ+ACEi/BB, n = 6; AS+TRZ+ACEi/BB, n = 7; AS+ISO+TRZ+ACEi/BB, n = 9). TRZ (Ontruzant) was administered at 6 mg/kg body weight intraperitoneally (ip) weekly for four weeks. Cardioprotective therapy consisted of captopril (ACEi) and bisoprolol (BB), administered at 20 mg/kg and 5 mg/kg, respectively, in the drinking water. One week after the final TRZ injection (T1), cardiac function was reassessed, and mice were sacrificed. The body weight, heart weight, and tibia lengths were measured. Hearts were dissected for histopathological and electron microscopy analyses, with additional samples frozen and stored for gene expression analyses.

2.2. Drug administration

ISO (isoprenaline hydrochloride, Monico S.p.A., Venice, Italy) was dissolved in saline and administered subcutaneously at a dose of 300 mg/kg body weight, twice daily for two consecutive days. TRZ (Ontruzant®) was freshly dissolved in saline and administered intraperitoneally to mice at a dosage of 6 mg/kg of body weight once a week for a maximum of four weeks. The cardioprotective therapy began on the same day as the first TRZ injection and continued until T1, covering a total of 4 weeks. The treatment consisted of a combination of captopril (an ACE inhibitor, ACEi) and bisoprolol (a beta-blocker, BB), administered at dosages of approximately 20 mg/kg and 5 mg/kg per day, respectively. These doses were adapted from established human heart failure regimens and scaled appropriately for rodents to ensure they are physiologic and non-toxic. The drugs were dissolved in distilled water and provided to the mice as drinking water, which was refreshed every two days. Water consumption was recorded to monitor actual drug intake, and concentrations were adjusted accordingly to maintain target dosages. In the Supplemental Material, data on the average daily water consumption for each experimental group treated with TRZ and the cardioprotective therapy over the four weeks of treatment are available. Additionally, it includes a table summarising the weekly and overall average dosages of captopril and bisoprolol administered to each group.

2.3. Echography and electrocardiography

Transthoracic echocardiography was performed using a Vevo 3100 ultrasound system (Vevo 3100, FUJIFILM VisualSonics Inc, Toronto,

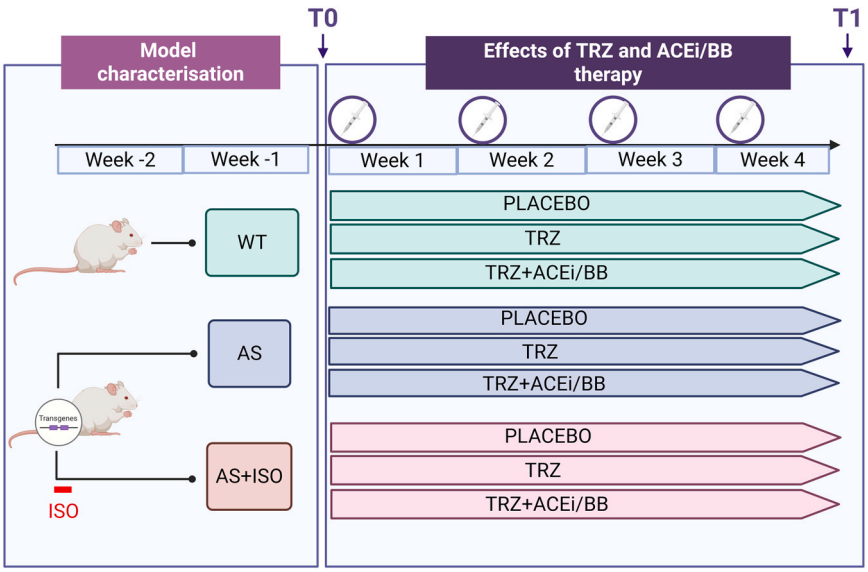

Fig. 1. Experimental design and treatment timeline in mice. *Model characterisation block* (Weeks −2 to −1, up to T0). WT: Wild-Type mice. AS: mice carrying aldosterone synthase transgenes to model cardiac hyperaldosteronism. AS+ISO: AS mice treated with ISO (red bar indicates ISO exposure). *Treatment Phase block* (Weeks 1–4, T0 to T1). Mice from each model group were assigned to one of the following treatment regimens: placebo; trastuzumab alone (TRZ); Combination of TRZ with ACE inhibitor and beta-blocker therapy (TRZ+ACEi/BB). Timeline Details: T0 = model characterisation or start of treatment interventions; T1 = end of treatment interventions; syringe icons indicate time points for TRZ or saline administration. Color coding: Green= WT mice groups; Blue= AS mice groups; Red: AS+ISO mice groups. Created with BioRender.com.

Canada) with a 40 MHz linear probe (MX 550S). Two-dimensional images were captured in parasternal long-axis and short-axis views, as well as transmitral inflow velocities via pulse–wave Doppler in the apical 4-chamber view. Images were analysed offline using the LV Trace software (FUJIFILM VisualSonics Inc., Toronto, Canada) to assess cardiac structure and function. Systolic and diastolic left ventricular (LV) volumes, stroke volume, ejection fraction (EF), fractional shortening (FS), LV mass, diastolic posterior wall and interventricular septum thickness (LVPWTd and IVSTd) were assessed. PW-Doppler images were used to evaluate diastolic and systolic function expressed as the early to late ventricular filling velocities (E/A) ratio.

A standard lead ECG was recorded using needle electrodes in sedated mice (1 % isoflurane in pure oxygen at a flow rate of 1 l/min) over a minimum of 5 min at a 4 kHz sampling rate with ML135 PowerLab/8SP equipped with Dual Bio Amp and MLA0112 ECG Lead Switch Box (ADI Instruments Ltd., Oxford, UK). Measurements included heart rate (HR), QRS duration, HR-corrected QT interval (QTc), and HR-corrected JT interval (JTc, an index of ventricular repolarisation). To ensure that the observed differences were not influenced by the possible circadian pattern of QT interval duration, we conducted all ECG measurements in the 8:00–9:30 a.m.

2.4. Assessment of tissue pathology score and mitochondrial damage

Cardiac tissues embedded in paraffin were sectioned and stained with hematoxylin-eosin and picrosirius red to assess pathology scores. Histological images (20x, 200x, and 400x) were acquired by a light microscope (Olympus BX43, Japan) and digitised with an RGB video camera (Olympus DP 20, Japan). Determination of cardiomyocyte cross-sectional area (CSA) was carried out at 400X magnification using a digital image analyser (CellSens, Olympus, Japan), following the details outlined in the Supplemental Material. Tissue sections were assessed for the severity of myocyte damage (including cell vacuolisation, myofibril disarray, cellular degeneration, and necrosis), interstitial damage (such as fibrosis and inflammatory infiltration), and perivascular fibrosis. Each parameter was scored on a semiquantitative scale from 0 to 3, and the scores were summed to determine the overall pathology score as detailed in the Supplemental Material. We also analysed cardiomyocyte ultrastructure and mitochondrial morphometry using transmission electron microscopy. Briefly, samples of left ventricles were processed as described in the Supplemental Material, and ultra-thin sections were examined with JEM-100 SX TEM (JEOL, Italia, S.p.A.). For mitochondrial analysis, we estimated volume density, defined as the volume of subcellular organelles per unit volume of tissue, which provides a quantitative marker of the organelles' ultrastructural alterations. We used the degree of mitochondrial swelling to score mitochondrial impairment according to the semi-quantitative impairment score outlined in the Supplemental Material.

For histological and electron microscopy analyses, tissues from both male and female mice were used; however, all comparisons within each figure panel were made using tissues from animals of the same sex to ensure consistency.

2.5. Assessment of the transcription levels of genes associated with cardiomyocyte survival and mitochondrial homeostasis

RNA was extracted from the left ventricle, then reverse transcribed and amplified as described in the Supplemental Material. Gene expression was quantified using custom-designed oligo primers purchased from Eurofins Genomics Italy (Milano, Italy). These primers targeted the following genes: B-cell lymphoma 2 (*Bcl2*), Bcl-2-associated X protein (*Bax*), Superoxide dismutase 2 (*Sod-2*), Peroxisome proliferator-activated receptor-gamma coactivator 1alpha (*Pgc-1α*), Mitofusin 2 (*Mfn-2*), Optic atrophy 1 (*Opa-1*), Dynamin-related protein (*Drp-1*), and Fission protein 1 (*Fis-1*). qPCR was performed with hypoxanthine phosphoribosyltransferase (*Hprt*) and hydroxymethylbilane synthase (*Hmbs*) as housekeeping controls. Relative quantification was carried out using Rotor Gene Q-Series Software. The primer sequences and PCR conditions are provided in the Supplemental Material.

2.6. Statistical analysis

Data were analysed with GraphPad Prism 9 version 9.5.0 (GraphPad Software, LLC). All data were tested for normality and presented as mean ± standard deviation (SD). Inter-group differences were examined by one-way or two-way ANOVA, as appropriate, and Tukey's multiple

comparison test. Tests were considered statistically significant when $p < 0.05$.

3. Results

The AS transgenic mice exhibited no signs of suffering, with growth and behaviour comparable to the WT strain. All WT mice reached the study endpoint. Two AS mice (1 female and 1 male) died during the protocol, accounting for 5 % of the group. Among 67 AS mice treated with ISO, 12 (5 females and 7 males) died during the two-day treatment. No additional deaths occurred in the AS+ISO group afterwards. Further information on body and heart weights and tibia lengths is detailed in the Supplemental Material.

3.1. Cardiac assessment in WT, AS, and AS+ISO mouse models

We characterised three models of different baseline cardiac impairments: healthy mice (WT), mice overexpressing cardiac aldosterone (AS), and AS mice challenged with ISO to develop overt cardiac dysfunction (AS+ISO). The body and heart weights of the three groups at T0 are reported in Supplemental Table S1. Supplemental Table S2 summarises the ultrasound-derived indices of cardiac function and morphology. The AS+ISO group showed a 25 % reduction in EF (46 ± 5 vs 62 ± 3 %, $p < 0.001$) compared to the WT group, and a decline of 22 % (46 ± 5 vs. 59 ± 5 %, $p < 0.001$) compared to the AS group (Fig. 2A). Both AS and AS+ISO mice had substantial increases in LV mass normalised to tibia length, with increases of 19 % and 28 %, respectively, compared to the WT group (6.3 ± 0.8 mg/mm in AS and 6.8 ± 0.8 mg/mm in AS+ISO vs. 5.3 ± 0.5 mg/mm in WT, $p = 0.005$ and $p < 0.001$) (Fig. 2B).

ECG analysis (Supplemental Table S2) revealed that the AS+ISO group had a longer QTc interval than the WT group (48 ± 2 ms and 45 ± 2 ms, respectively, $p = 0.041$) (Fig. 2C). No variations in the QRS interval were detected, indicating that the longer QTc was primarily due to an extended repolarisation phase, evidenced by a longer JTc interval in AS+ISO mice (39 ± 2 ms) compared to both WT mice (36 ± 2 ms, $p = 0.006$) and AS mice (37 ± 2 ms, $p = 0.016$) (Fig. 2D).

The histopathological analysis revealed an overall preservation of myocardial organisation across all groups. However, the AS+ISO group exhibited significant myocardial damage, with a pathological score of 2.6 ± 0.89 compared to 0.2 ± 0.44 in WT and 0.88 ± 0.62 in AS ($p < 0.001$ and $p = 0.008$, respectively). This damage included inflammatory cell infiltration, often arranged in focal clusters, increased perivascular fibrosis in epicardial arteries (Fig. 2E), and focal collagen deposition between cardiomyocytes (Fig. 2F). Moving from the WT to the AS and AS+ISO groups, mice exhibited an increase in CSA. In WT mice, average CSA was 216 ± 6 μm^2, while in AS it was 15 % higher (248 ± 19 μm^2; $p < 0.015$), and 25 % higher (271 ± 19 μm^2) in AS+ISO ($p < 0.001$ compared to WT and $p = 0.071$ compared to AS). The ultrastructure of cardiomyocytes in WT was regular, characterised by uniform mitochondria in size and shape, with well-defined cristae and a dense matrix (Fig. 2G). In the AS mice, we observed a few mildly swollen mitochondria that showed a slight increase in size but maintained an almost regular cristae pattern and matrix density. However, the AS+ISO group displayed many damaged mitochondria, with displaced cristae and a dispersed matrix. Quantitative analysis showed a significantly increased volume density of mitochondria in the AS+ISO group compared to WT mice (29.6 ± 2.3 vs. 21.4 ± 3.8, $p < 0.001$). Swollen mitochondria were observed only in the AS (2.5 %) and AS+ISO (5.6 %) groups ($p < 0.05$ and $p < 0.001$ vs. WT, respectively), Fig. 2H.

These changes were accompanied by altered expression of genes related to cardiomyocyte survival and function, as well as mitochondrial quality control (Fig. 3). The expression levels of pro-apoptotic (*Bax*) and anti-apoptotic (*Bcl-2*) genes and the *Bax/Bcl-2* ratio showed no significant differences between the WT and AS groups. However, in the AS+ISO mice, *Bcl-2* expression increased by over 1.5-fold, and the *Bax* expression rose by approximately 6-fold compared to the WT and AS mice. The *Bax/Bcl-2* ratio increased 4.2-fold, highlighting the dominance of pro-apoptotic signals in the AS+ISO mice ($p < 0.001$ vs. both groups). Additionally, mitochondrial *Sod-2* expression showed a trend towards reduction in the AS group, but it declined significantly in AS+ISO mice ($p < 0.001$ vs. WT), suggesting impaired oxidative stress protection in this group. Moreover, AS+ISO mice showed significant downregulation of *Pgc–1α* ($p < 0.001$ vs. WT and AS), a critical mediator for cellular processes and mitochondrial homeostasis.

Regarding mitochondrial dynamics, we observed a 24 % downregulation of mitochondrial fusion gene *Mfn-2* compared to the WT group ($p = 0.016$) in the absence of changes in the transcriptional levels of fission-related genes (*Drp-1* and *Fis-1*). AS+ISO mice showed a 36 % reduction in the expression of the fusion-related gene Opa-1 compared to WT ($p < 0.001$). AS+ISO mice also exhibited increased transcriptional levels of fission-related genes *Drp-1* and *Fis-1* ($p < 0.001$ and $p < 0.003$ vs. WT). These findings indicate that impaired mitochondrial dynamics and quality render AS mice more vulnerable to mitochondrial damage than WT mice. This condition worsens under adrenergic stress in the AS+ISO group.

3.2. Trastuzumab induced cardiac impairment and the combined ACEi and BB therapy prevented TRZ-induced effects on cardiac function and electrical activity

Body and heart weights of all groups are reported in Supplemental Table S3. The main parameters from the US and ECG analysis run at T1 are summarised in Supplemental Table S4. TRZ reduced systolic function by 8–10 % compared to placebo-treated mice across all groups, as measured by EF ($p < 0.01$ compared to the corresponding PBO in all groups) (Fig. 4A**)**. However, the ACEi/BB therapy preserved systolic function in both WT and AS mice treated with TRZ, maintaining EF at 63 ± 2 % and 59 ± 2 %, respectively ($p < 0.001$ versus their corresponding TRZ groups). In the AS+ISO+TRZ+ACEi/BB group, this therapy prevented the EF reduction ($p < 0.001$ compared to the AS+ISO+TRZ) and even improved systolic performance compared to the AS+ISO+PBO group ($p < 0.001$).

In WT mice, TRZ significantly increased the QTc interval to 51 ± 4 ms compared to 47 ± 4 ms in the WT+PBO group ($p = 0.002$) (Fig. 4B). This increase was primarily due to a prolonged JTc of 42 ± 3 ms in the TRZ group versus 37 ± 4 ms in the WT+PBO mice ($p = 0.003$) (Fig. 4C). In the AS and AS+ISO groups, which already had prolonged ventricular electrical activity at T0, TRZ did not cause further increases of QTc or JTc. QTc and JTc intervals of mice administered with ACEi/BB therapy were shorter across all groups than their respective TRZ and placebo treatments.

3.3. Cardioprotective therapy improved TRZ-induced alterations in cardiac tissue

All TRZ-treated groups showed inflammatory cell infiltration, with similar prevalence (Fig. 5A). Mice in the WT+TRZ and AS+TRZ groups exhibited sporadic foci of cytotoxic lesions with myocardial vacuolisation and disorganised myofibrils (Fig. 5B). In contrast, the AS+ISO+TRZ group displayed more frequent signs of cardiomyocyte degeneration and inflammatory aggregates (Fig. 5C). Picrosirius red staining revealed increased perivascular and spotty interstitial reparative fibrosis, especially in the trabecular tissue and subendocardial regions (Fig. 5D). Histopathology showed that TRZ significantly raised pathology scores in all groups compared to PBO treatments, with WT and AS mice scoring 2.1 ± 0.7 and 2.4 ± 0.9 ($p = 0.011$ and $p = 0.003$, respectively).

AS+ISO mice significantly increased from 2.8 ± 1.5 with PBO to 5.2 ± 1.2 after TRZ ($p < 0.001$). ACEi/BB therapy protected mice from TRZ-induced tissue remodelling, reducing inflammatory cell infiltrates across all groups (Fig. 5E). In the AS+ISO mice, the cardioprotective therapy also effectively reduced perivascular and interstitial fibrosis (Fig. 5F).

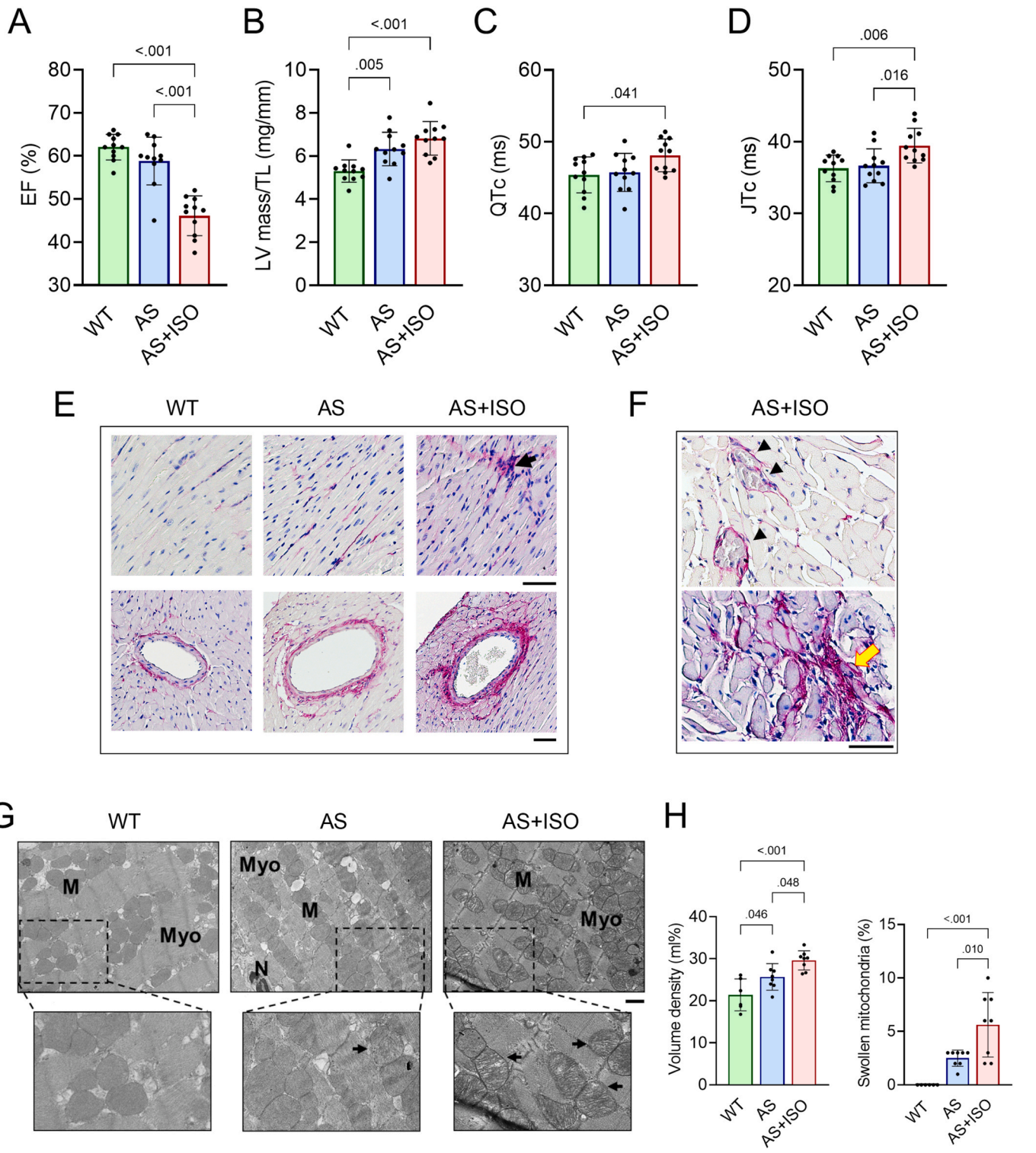

Fig. 2. LV function and electrical activity, myocardial histopathology and mitochondrial morphometry at T_0. (A) Ejection fraction (EF) percentage. (B) Left ventricular mass normalised to tibia length. (C) QT interval corrected for heart rate (QTc). (D) JT interval corrected for the heart rate (JTc). (E) Recruitment of mononuclear cells in the tissue (black arrow) in the upper panels, and sections showing epicardial coronary arteries in the lower panels. AS+ISO group showed abundant interstitial and perivascular fibrosis compared to the other groups (collagen is red). (F) Myocardial damage in the AS+ISO mice: Degenerated fragments of cardiomyocytes digested by inflammatory cell aggregates (black arrowheads) (upper); focal lesion with mononuclear cell infiltrates and interstitial collagen deposition (yellow arrow) (lower). Scale bar, 50 μm for all. (G) Progressive mitochondrial alteration from WT to AS and AS+ISO mice. Enlargements: arrows point to mitochondria with cristae derangement. M: mitochondria; Myo: myofibrils; N: nucleus. Scale bar: 1μm. (H) Quantitative analysis of mitochondria volume density and swelling. Representative histological and electron microscopy images shown are from female mice. Histograms: WT (green), AS (blue), and AS+ISO (red) groups. Data are mean ± SD, n = 11 mice/group in panels A-D and n = 6–8 mice/group in panels E-H.

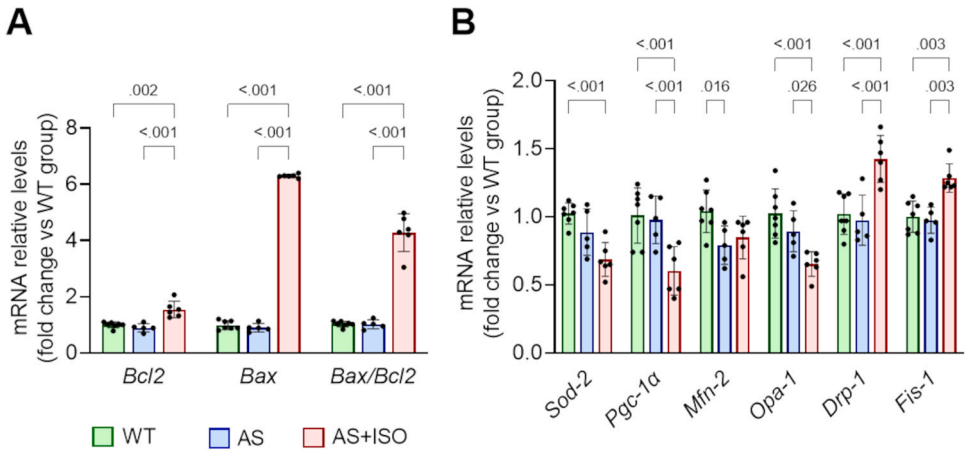

Fig. 3. Cardiomyocyte gene expression pattern. (A and B) RT-PCR quantification of genes linked to cell survival (*Bcl-2* and *Bax*), cellular function (*Sod-2* and *Pgc-1α*), and mitochondrial dynamics (*Mfn-2*, *Opa-1*, *Drp-1* and *Fis-1*). Gene expression was normalised to the messenger RNA (mRNA) of WT mice. Values are mean ± SD, n = 5–7 mice/group.

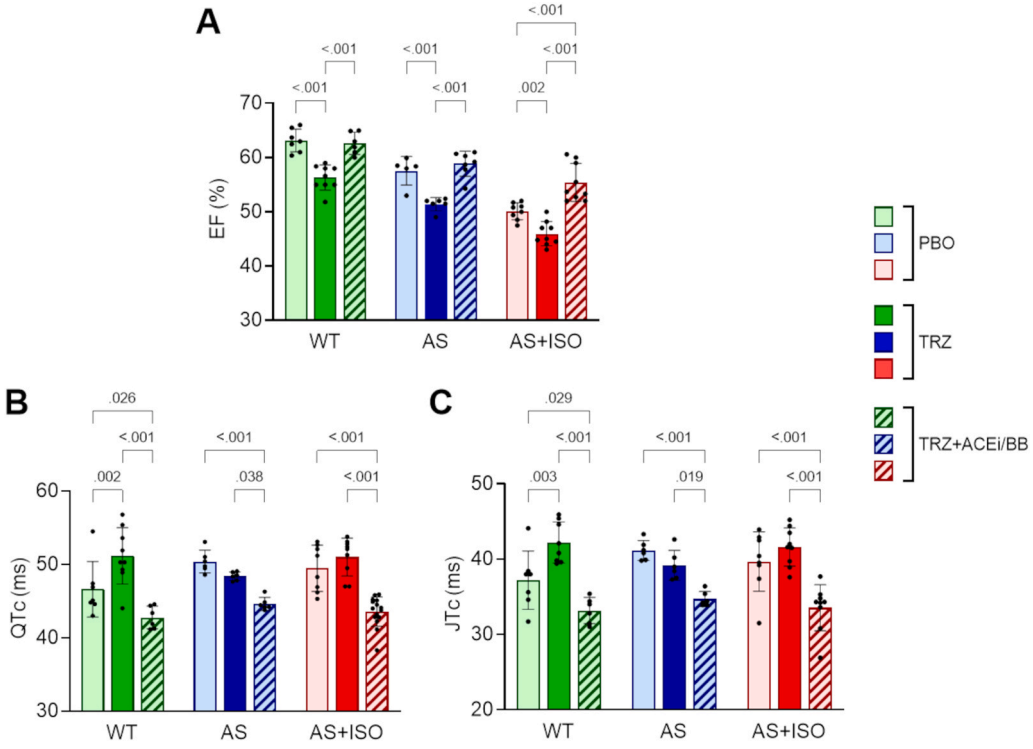

Fig. 4. Effect of ACEi and BB therapy on cardiac function and electrical activity in TRZ-treated mice. (A) Ejection fraction (EF) percentage. (B) QT interval corrected for heart rate (QTc). (C) JT interval corrected for heart rate (JTc). Groups: WT (green bar), AS (blue), and AS+ISO (red bar). Treatments: PBO (light colour), TRZ (dark colour), and TRZ+ACEi/BB (pattern) in all groups. Data are mean ± SD, with n = 6–8 mice in each group.

Pathology scores improved across groups: 0.8 ± 0.4 in WT+TRZ+ACEi/BB, 1.6 ± 0.6 in AS+TRZ+ACEi/BB, and 2.3 ± 0.6 in AS+ISO+TRZ+ACEi/BB mice ($p < 0.001$ vs. AS+ISO+TRZ). Fig. 5G shows that in WT mice, TRZ led to a 24 % increase in CSA compared to PBO (265 ± 18 μm^2 vs. 219 ± 5 μm^2, $p < 0.001$). AS and AS+ISO mice showed increases of 14 % (267 ± 7 μm2 vs. 233 ± 13 μm2, $p < 0.001$) and 8 % (308 ± 15 μm^2 vs. 284 ± 16 μm^2, $p = 0.006$), respectively. However, ACEi/BB therapy counteracted the increase in CSA across all groups. In the WT+TRZ+ACEi/BB group, CSA decreased to 240 ± 9 μm^2 ($p = 0.008$ vs. WT+TRZ). AS+TRZ+ACEi/BB mice had CSA values of 250 ± 6 μm^2 ($p = 0.04$ vs. AS+TRZ). In the AS+ISO+TRZ+ACEi/BB group, the CSA was reduced to 250 ± 7 μm^2 ($p < 0.001$ vs. AS+ISO+TRZ), a value even lower compared to the AS+ISO+PBO group ($p < 0.001$).

3.4. Combined ACEi/BB therapy mitigates cardiac ultrastructure impairment induced by TRZ

All TRZ-treated groups exhibited structural abnormalities in mitochondria, despite a generally preserved cellular organisation compared to the PBO groups. Mitochondria showed an increased average size relative to the corresponding placebo and alterations in the matrix and cristae. Fig. 6A highlights moderate to severe mitochondrial morphological impairment progressing from WT to AS and AS+ISO groups. In WT+TRZ and AS+TRZ mice, some cardiomyocytes presented slight mitochondrial size increases, with some showing dispersed matrix and

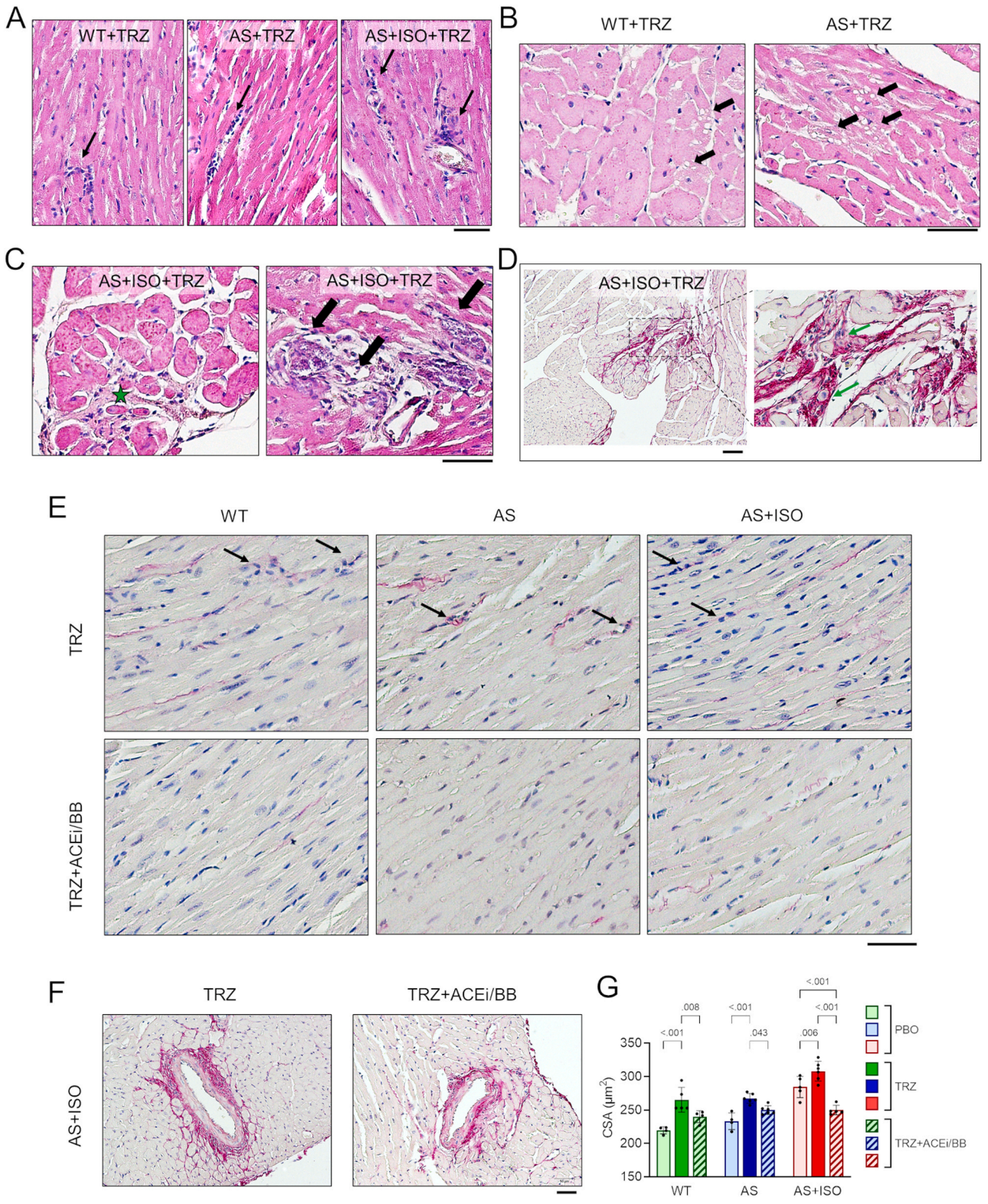

Fig. 5. Histopathology of cardiac tissue in TRZ-treated mice of the three groups and effect of ACEi and BB therapy in TRZ-treated mice. (A) interstitial cellular infiltrate (black arrows). (B) damaged cardiomyocytes with cellular vacuolisation and myofibril derangement (black arrows). (C) Sign of healing process with mononuclear cell infiltrates (green star) and inflammatory cell aggregates containing degenerated cardiomyocyte fragments (black arrows). (D) reparative fibrosis. Enlargement: degenerated cardiomyocytes surrounded by mononuclear cell infiltrates (green arrows) and collagen (red staining). (E) Cardioprotective therapy reduced the inflammatory cell infiltrates (black arrows) and collagen fibres (red staining). (F) Cardioprotective therapy reduced perivascular collagen deposition (red staining). Scale bars: 50μm (A-C, E); 100μm (D). Representative histological images shown are from male mice. (G) Cardiomyocytes' cross-sectional area. The histogram's caption is as in Fig. 4. Data are mean ± SD, n = 4–6.

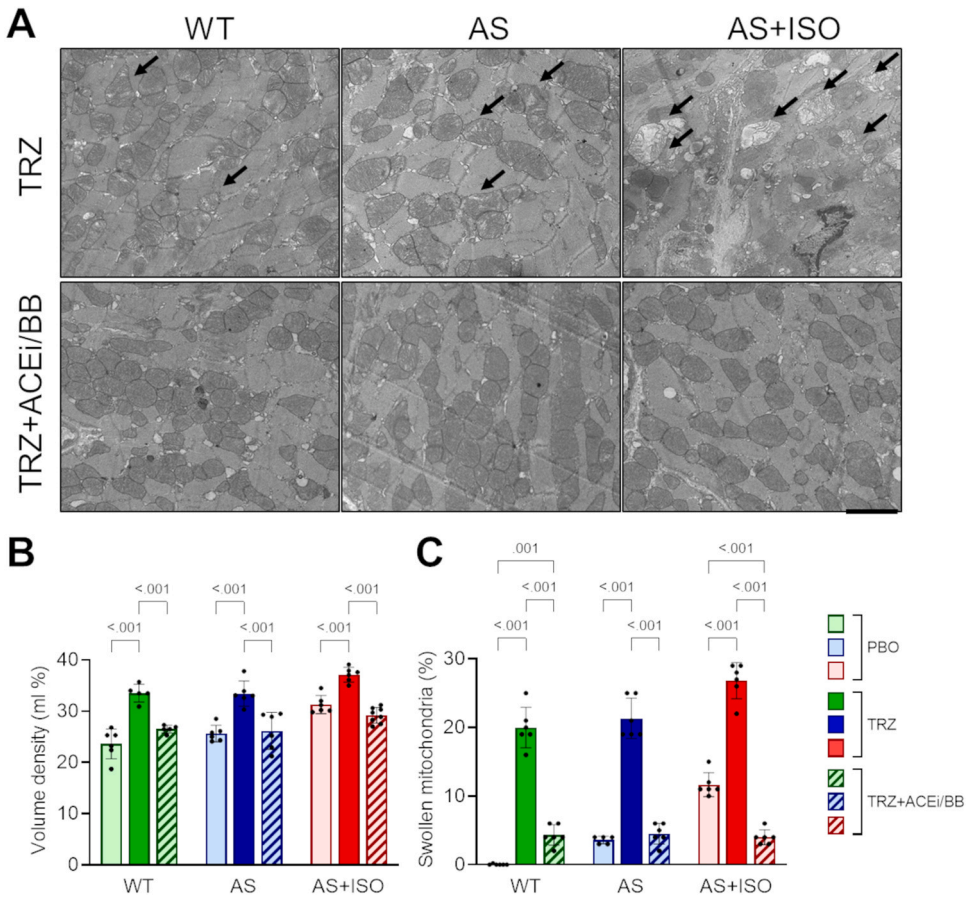

Fig. 6. Effect of ACEi and BB therapy on mitochondria in TRZ-treated mice (A) mitochondria showed swelling and dilated or fragmented cristae (black arrows) in all groups treated with TRZ. Recovered morphology in the TRZ+ACEi/BB mice. Scale bar: 2μm. Representative electron microscopy images shown are from male mice. (B and C) Quantitative analysis of mitochondria volume density and swelling. The histogram's caption as in Fig. 4. Data are mean ± SD, n = 5–7.

dilated or fragmented cristae. Many cardiomyocytes of AS+ISO+TRZ exhibited heavily dilated organelles with disrupted cristae and dispersed matrix. Mice treated with TRZ showed increased mitochondrial volume density and a higher percentage of swollen mitochondria compared to those receiving PBO and TRZ+ACEi/BB treatments ($p < 0.001$ in all groups compared to those receiving PBO and TRZ+ACEi/BB), as

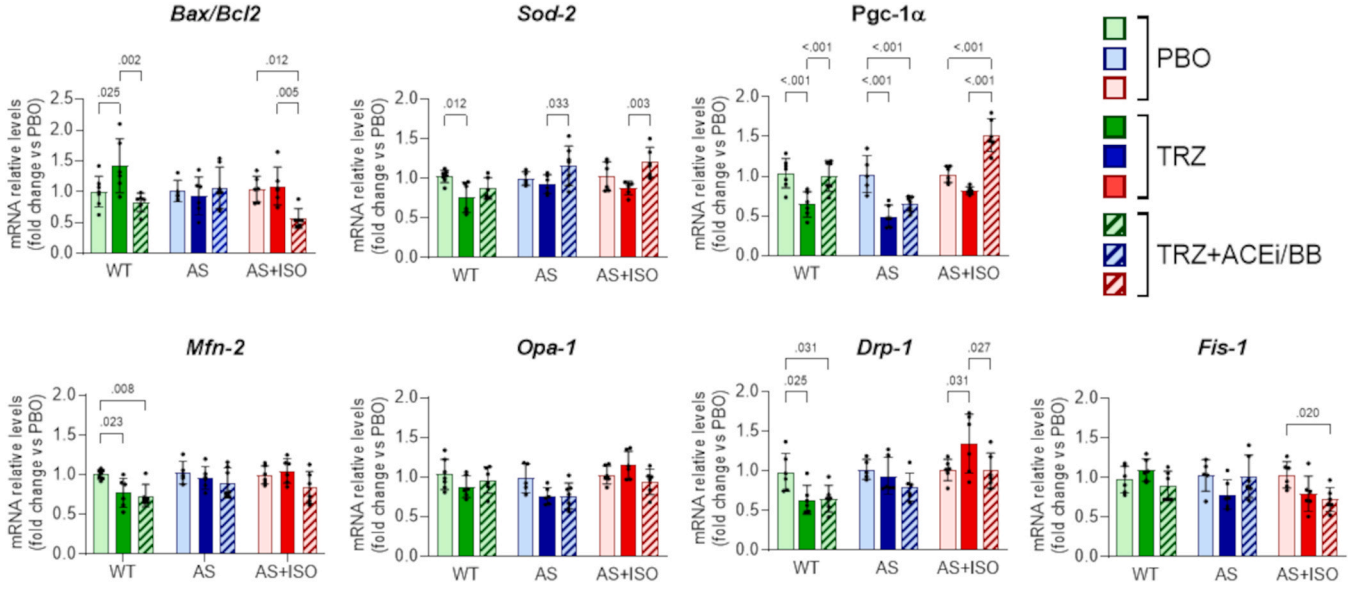

Fig. 7. Cardiomyocyte gene expression pattern. RT-PCR quantification of genes linked to cell survival (*Bcl2* and *Bax*), cellular function (*Sod-2* and *Pgc-1α*), and mitochondrial dynamics (*Mfn-2*, *Opa-1*, *Drp-1,* and *Fis-1*) in cardiac tissue. Gene expression was normalised to PBO mice of each group. The histogram's caption as in Fig. 4. Data are mean ± SD, n = 5–7.

illustrated in Fig. 6B-C.

Mitochondrial pathology scores for TRZ-treated WT and AS groups were significantly higher (score 3) compared to their PBO counterparts (scored 0.33 and 1, respectively, $p < 0.001$ for both). The AS+ISO+TRZ group scored 3.8 compared to 2 for the AS+ISO+PBO group ($p < 0.001$). With ACEi/BB therapy, pathology scores improved significantly in all groups: 1.25 for WT+TRZ+ACEi/BB, 1.5 for AS+TRZ+ACEi/BB, and 1.13 for AS+ISO+TRZ+ACEi/BB group, respectively ($p < 0.001$ vs.TRZ-treated groups).

Fig. 7 displays the *Bax/Bcl-2* ratio and the relative expression levels of *Pgc-1α*, *Sod-2*, *Drp-1*, *Fis-1*, *Mfn-2*, and *Opa-1*. WT mice showed a 1.4-fold increase in the *Bax/Bcl-2* ratio after TRZ compared to the WT+PBO group ($p = 0.025$), which was completely prevented in the WT+TRZ+ACEi/BB group ($p = 0.002$ vs. WT+TRZ). AS+ISO mice, with a higher *Bax/Bcl-2* ratio at T0 than the other groups, showed no further changes post-TRZ. However, they achieved a 40 % reduction in the ratio with concurrent cardioprotective therapy ($p = 0.005$ vs. AS+ISO+TRZ and $p = 0.012$ vs. AS+ISO+PBO). *Sod-2* expression declined in all TRZ-treated groups, significantly in the WT +TRZ group ($p = 0.012$ vs. WT+PBO). However, combining cardioprotective therapy with TRZ restored *Sod-2* transcription levels in the WT+TRZ+ACEi/BB mice and significantly improved levels in AS+TRZ+ACEi/BB and AS+ISO+TRZ+ACEi/BB groups ($p = 0.033$ and $p = 0.003$ vs. TRZ-treated mice, respectively). Hearts from mice treated with TRZ showed downregulation of *Pgc–1α*, a key mediator of mitochondrial quality control and cellular hypertrophy, with a 35 % decrease in WT+TRZ group and 50 % in AS+TRZ group ($p < 0.001$ vs. PBO groups for both). The AS+ISO+TRZ group experienced a 20 % decrease, which was not significantly different from that of the placebo group. Cardioprotective therapy significantly restored gene transcription levels in the WT+TRZ+ACEi/BB and AS+ISO+TRZ+ACEi/BB groups ($p < 0.001$ vs. TRZ-treated groups for both). Notably, it also improved the transcription levels compared to those measured at T0 in the AS+ISO model. Regarding mitochondrial dynamics processes, TRZ reduced *Mfn-2* transcription in WT mice by 25 % and *Drp-1* by 35 %, while *Opa-1* and *Fis-1* levels remained unchanged. However, in AS+ISO mice that showed decreased transcription levels of mitochondrial fusion genes and increased levels of fission genes at T0 compared to the other groups, TRZ did not significantly alter *Mfn-2*, *Opa-1* and *Fis-1*. However, *Drp-1* transcription levels rose by about 35 % compared to the AS+ISO+PBO group ($p = 0.031$). Combining TRZ with cardioprotective therapy normalised *Drp-1* levels ($p = 0.027$ vs. AS+ISO+TRZ). Additionally, ACEi/BB therapy reduced *Fis-1* levels by about 25 % compared to the AS+ISO+PBO group ($p = 0.02$). These findings indicate that TRZ in this group further disrupts the balance between mitochondrial fission and fusion, an effect that cardioprotective therapy effectively mitigates.

4. Discussion

Our study indicates: a) that TRZ leads to significant cardiac impairment both in a mouse model with normal cardiac function and in two models with pre-existing overt cardiac dysfunction and with cardiac overexpression of aldosterone; b) that an established cardioprotective treatment with combined ACEi/BB effectively prevents TRZ-induced cardiotoxicity, improving cardiac function and structure even in animals with pre-existing overt cardiac dysfunction.

These findings enhance our understanding of the impact of HER2-targeted treatments, such as TRZ, in the clinical setting, specifically in patients with pre-existing cardiac dysfunction, which is known to increase the risk of cardiotoxicity. However, clinical trials have only recently begun to address this subgroup.

4.1. Mouse models of TRZ cardiotoxicity

A moderate decline in cardiac function in WT mice following TRZ has been confirmed in multiple studies [11,13–15], along with structural and ultrastructural changes in myocardial tissue [10,14,15]. Studies have also reported the activation of apoptotic pathways following treatment with TRZ [10,14,24,25]. In line with these findings, our observations revealed diminished cardiac function and the presence of inflammatory cell infiltration in myocardial tissue across all studied groups. Cellular vacuolisation and sporadic necrotic or degenerating cardiomyocytes were observed in a few WT and AS individuals, representing the low- and moderate-risk populations, and more prominently in the AS+ISO group after TRZ. Furthermore, TRZ-induced fibrotic lesions were primarily observed in AS+ISO mice and occasionally in the AS group. While the TRZ-induced cardiotoxicity entails complex and still partially unknown mechanisms, mitochondrial dysfunction appears to play a key role in the transition from health to disease [26]. Mitochondrial integrity is crucial for energy metabolism, calcium homeostasis, and ROS production. Our findings indicated varying degrees of mitochondrial damage in cardiomyocytes across all groups, consistent with TRZ-related cardiotoxicity previously observed in healthy mice [10,14,15,27]. The percentage of altered mitochondria across the three groups after TRZ varied based on baseline mitochondrial homeostasis. Before treatment, the number of damaged mitochondria was lower in the WT and AS groups than in the AS+ISO group. This ultrastructural condition was compatible with compromised cardiomyocytes, still within viable tissue, though some cells showed signs of potential apoptosis or necrosis, as confirmed by histopathological data. Differences in gene transcription related to cardiomyocyte survival and mitochondrial quality control further highlighted the distress of cardiomyocytes among groups. AS+ISO mice exhibited upregulated pro-apoptotic pathways and downregulated protective mechanisms against oxidative stress and *Pgc–1α*, a crucial mediator of mitochondrial homeostasis and metabolic processes. While AS mice showed a moderate decrease in transcription levels of mitochondrial fusion genes, AS+ISO mice displayed a significant shift toward fission, thereby increasing the risk of mitochondrial damage. The increased severity and prevalence of cellular damage in AS+ISO mice were likely due to the inhibition of HER2-mediated survival signalling in a previously compromised myocardial tissue, as indicated by the altered gene expression levels measured at T0. No prior studies have investigated the effects of TRZ or other cancer therapies in models with pre-existing cardiac impairment, suggesting these findings provide new insights beyond those established in previous animal studies.

Moreover, the murine model employed in the present study, i.e. cardiac-specific hyperaldosteronism receiving subcutaneous isoproterenol injections to induce LV systolic dysfunction, is associated with diffuse myocardial damage and cardiac hyperaldosteronism, in the absence of discrete myocardial infarction or afterload increase, as for the case of coronary artery ligation and transverse aortic constriction, respectively, thus resembling clinical nonischemic dilated cardiomyopathy commonly observed in patients receiving cardiotoxic drugs.

4.2. Combined ACEi/BB therapy in the primary prevention of TRZ-induced cardiotoxicity

The use of cardioprotective strategies, including beta-blockers and ACE inhibitors, in patients undergoing anti-cancer therapies remains a topic of debate [28–30]. While these medications are recommended for high-risk patients, their role in asymptomatic individuals remains uncertain, questioning the routine use of ACE inhibitors and beta-blockers for the primary prevention of cardiotoxicity. Our study highlights the importance of cardiac monitoring and cardioprotective therapy for individuals receiving TRZ treatment. In WT and AS mice, considered at low cardiac risk, the concomitant administration of ACEi/BB therapy effectively prevented TRZ-induced cardiotoxicity. Interestingly, in AS+ISO mice, cardioprotective treatment not only prevented TRZ-related toxicities, but the TRZ+ACEi/BB group outperformed the placebo group in many of these hallmarks. These findings suggest that the ACEi/BB co-administration provides benefits beyond primary

prevention. Our study chose a combination of bisoprolol and captopril as a cardioprotective therapy. Bisoprolol is a third-generation beta-blocker with antioxidant, anti-apoptotic, and anti-inflammatory properties demonstrated both in vivo and in vitro [31,32]. Bisoprolol preserved systolic function and myocardial ultrastructure in a rat model of DOX cardiotoxicity [33], but its effects on TRZ-induced cardiotoxicity remain unexplored. Captopril, a thiol-containing ACE inhibitor, also showed protective antioxidant, anti-inflammatory, anti-apoptotic, and anti-hypertrophic effects in animal models of myocardial injury [34–36]. Despite these findings, some studies have shown conflicting results regarding captopril effects on mitochondria [37–39]. However, consistent with our findings, a recent study by El-Sayed et al. revealed that captopril enhances cardiac function and remodelling in rats treated with ISO by modulating mitochondrial homeostasis, promoting mitochondrial fusion while reducing fission [40].

4.3. Study limitations

Our preclinical model of TRZ treatment may not accurately reflect clinical scenarios, particularly regarding the administration schedule of TRZ and its combination with other drugs. Moreover, the absence of a tumoral background in our murine models may oversimplify the complex interactions between cancer, therapies, and cardiovascular function. Additionally, our findings require a deeper understanding of the molecular mechanisms to better interpret the cardiotoxic effects of TRZ and responses to cardioprotective treatments. Moreover, our study employed a combined therapy with an ACE inhibitor and a beta-blocker, without evaluating each drug individually. As a result, the specific benefits and mechanisms of action of each drug remain uncertain. This will be an important focus for future targeted studies. Furthermore, while our findings did not reveal significant sex-based effects, the sample size was limited for stratified analyses. Future studies specifically designed and powered to evaluate sex differences will be essential to address this important question fully.

5. Conclusions

Treatment with TRZ induces cardiac dysfunction and alters cardiac structure and ultrastructure, regardless of pre-existing cardiac issues. However, the most severe phenotype is observed in mice with prior cardiac impairment linked to likely increased frailty. Our results provide evidence that the concurrent administration of captopril and bisoprolol effectively mitigates the harmful effects of TRZ on the heart in mouse models with and without baseline cardiac dysfunction. Cardioprotective therapy improves LV systolic function and counteracts detrimental changes in mitochondrial morphology and the altered transcriptional signature relevant to mitochondrial biology in murine models of TRZ-induced cardiotoxicity.

CRediT authorship contribution statement

Serena L'Abbate: Writing – original draft, Investigation, Formal analysis, Conceptualization. **Claudia Kusmic:** Writing – original draft, Project administration, Investigation, Funding acquisition, Formal analysis, Conceptualization. **Vincenzo De Tata:** Writing – review & editing, Investigation, Formal analysis. **Michele Emdin:** Writing – review & editing, Conceptualization. **Iacopo Fabiani:** Writing – review & editing, Formal analysis. **Giuseppe Vergaro:** Writing – review & editing, Investigation, Formal analysis. **Sabrina Marchetti:** Writing – review & editing, Investigation, Formal analysis. **Francesca Forini:** Writing – review & editing, Investigation, Formal analysis. **Matilde Masini:** Writing – review & editing, Investigation, Formal analysis. **Giuseppina Nicolini:** Writing – review & editing, Investigation, Formal analysis.

Funding

This work was supported by a grant from Consiglio Nazionale delle Ricerche (CNR, Italy), grant number DSB.AD007.247, CUP B55F21003380007, to C.K.

Declaration of Competing Interest

The authors declare that they have no known competing financial interests or personal relationships that could have appeared to influence the work reported in this paper.

Acknowledgements

The authors would like to thank Dr. Chiara Rossi for her support with digital PCR analysis, and Dr. Michela Novelli for her assistance with the electron microscopy facility. Additionally, the authors acknowledge Mrs. Cecilia Ciampi and Ms. Sara Ciampi for their invaluable support in animal care.

Appendix A. Supporting information

Supplementary data associated with this article can be found in the online version at doi:10.1016/j.biopha.2025.118490.

Data availability

Data will be made available on request.

References

[1] M. Vaduganathan, G.A. Mensah, J.V. Turco, V. Fuster, G.A. Roth, The global burden of cardiovascular diseases and risk: a compass for future health, J. Am. Coll. Cardiol. 80 (2022) 2361–2371, https://doi.org/10.1016/j.jacc.2022.11.005.
[2] N.M.L. Battisti, C.A. Welch, M. Sweeting, M. de Belder, J. Deanfield, C. Weston, et al., Prevalence of cardiovascular disease in patients with potentially curable malignancies: a national registry dataset analysis, JACC CardioOncology 4 (2022) 238–253, https://doi.org/10.1016/j.jaccao.2022.03.004.
[3] M.A. Mamas, A. Matetic, How common is Pre-Existing cardiovascular disease in cancer patients: what do we know? Does it matter? JACC CardioOncology 4 (2022) 254–257, https://doi.org/10.1016/j.jaccao.2022.05.001.
[4] N. Dempsey, A. Rosenthal, N. Dabas, Y. Kropotova, M. Lippman, N.H. Bishopric, Trastuzumab-induced cardiotoxicity: a review of clinical risk factors, pharmacologic prevention, and cardiotoxicity of other HER2-directed therapies, Breast Cancer Res Treat. 188 (2021) 21–36, https://doi.org/10.1007/s10549-021-06280-x.
[5] K. Lemmens, K. Doggen, G.W. De Keulenaer, Role of neuregulin-1/ErbB signaling in cardiovascular physiology and disease: implications for therapy of heart failure, Circulation 116 (2007) 954–960, https://doi.org/10.1161/CIRCULATIONAHA.107.690487.
[6] D. Meyer, C. Birchmeier, Multiple essential functions of neuregulin in development, Nature 378 (1995) 386–390, https://doi.org/10.1038/378386a0.
[7] S.A. Crone, Y.Y. Zhao, L. Fan, Y. Gu, S. Minamisawa, Y. Liu, et al., ErbB2 is essential in the prevention of dilated cardiomyopathy, Nat. Med 8 (2002) 459–465, https://doi.org/10.1038/nm0502-459.
[8] C. Özcelik, B. Erdmann, B. Pilz, N. Wettschureck, S. Britsch, N. Hübner, et al., Conditional mutation of the ErbB2 (HER2) receptor in cardiomyocytes leads to dilated cardiomyopathy, Proc. Natl. Acad. Sci. USA 99 (2002) 8880–8885, https://doi.org/10.1073/pnas.122249299.
[9] C. Fedele, G. Riccio, C. Coppola, A. Barbieri, M.G. Monti, C. Arra, et al., Comparison of preclinical cardiotoxic effects of different ErbB2 inhibitors, Breast Cancer Res Treat. 133 (2012) 511–521, https://doi.org/10.1007/s10549-011-1783-9.
[10] M.K. ElZarrad, P. Mukhopadhyay, N. Mohan, E. Hao, M. Dokmanovic, D.S. Hirsch, et al., Trastuzumab alters the expression of genes essential for cardiac function and induces ultrastructural changes of cardiomyocytes in mice, PLoS One 8 (2013), https://doi.org/10.1371/journal.pone.0079543.
[11] G. Milano, A. Raucci, A. Scopece, R. Daniele, U. Guerrini, L. Sironi, et al., Doxorubicin and trastuzumab regimen induces biventricular failure in mice, J. Am. Soc. Echocardiogr. 27 (2014) 568–579, https://doi.org/10.1016/j.echo.2014.01.014.
[12] C. Coppola, G. Riccio, A. Barbieri, M.G. Monti, G. Piscopo, D. Rea, et al., Antineoplastic-related cardiotoxicity, morphofunctional aspects in a murine model: contribution of the new tool 2D-speckle tracking, Onco Targets Ther. 9 (2016) 6785–6794, https://doi.org/10.2147/OTT.S106528.
[13] C. Altomare, A.M. Lodrini, G. Milano, V. Biemmi, E. Lazzarini, S. Bolis, et al., Structural and electrophysiological changes in a model of cardiotoxicity induced

by anthracycline combined with trastuzumab, Front Physiol. 12 (2021), https://doi.org/10.3389/fphys.2021.658790.
[14] J. Min, L. Wu, Y. Liu, G. Song, Q. Deng, W. Jin, et al., Empagliflozin attenuates trastuzumab-induced cardiotoxicity through suppression of DNA damage and ferroptosis, Life Sci. 312 (2023), https://doi.org/10.1016/j.lfs.2022.121207.
[15] A.M. Kabel, A.A. Elkhoely, Targeting proinflammatory cytokines, oxidative stress, TGF-β1 and STAT-3 by rosuvastatin and ubiquinone to ameliorate trastuzumab cardiotoxicity, Biomed. Pharm. 93 (2017) 17–26, https://doi.org/10.1016/j.biopha.2017.06.033.
[16] G. Curigliano, D. Lenihan, M. Fradley, S. Ganatra, A. Barac, A. Blaes, et al., Management of cardiac disease in cancer patients throughout oncological treatment: ESMO consensus recommendations, Ann. Oncol. 31 (2020) 171–190, https://doi.org/10.1016/j.annonc.2019.10.023.
[17] A.R. Lyon, T. López-Fernánde, L.S. Couch, R. Asteggiano, M.C. Aznar, J. Bergler-Klei, et al., 2022 ESC guidelines on cardio-oncology developed in collaboration with the european hematology association (EHA), the european society for therapeutic radiology and oncology (ESTRO) and the international Cardio-Oncology society (IC-OS), Eur. Heart J. 43 (2022) 4229–4361, https://doi.org/10.1093/eurheartj/ehac244.
[18] F. Lynce, A. Barac, X. Geng, C. Dang, A.F. Yu, K.L. Smith, et al., Prospective evaluation of the cardiac safety of HER2-targeted therapies in patients with HER2-positive breast cancer and compromised heart function: the SAFE-HEaRt study, Breast Cancer Res Treat. 175 (2019) 595–603, https://doi.org/10.1007/s10549-019-05191-2.
[19] D.P. Leong, T. Cosman, M.M. Alhussein, N. Kumar Tyagi, S. Karampatos, C. C. Barron, et al., Safety of continuing trastuzumab despite mild cardiotoxicity: a phase I trial. In, JACC CardioOncology (2019) 1–10, https://doi.org/10.1016/j.jaccao.2019.06.004.
[20] A. Asnani, J.J. Moslehi, B.B. Adhikari, A.H. Baik, A.M. Beyer, R.A. De Boer, et al., Preclinical models of cancer Therapy-Associated cardiovascular toxicity: a scientific statement from the American heart association, Circ. Res. 129 (2021) E21–E34, https://doi.org/10.1161/RES.0000000000000473.
[21] G. Vergaro, M. Prud'Homme, L. Fazal, R. Merval, C. Passino, M. Emdin, et al., Inhibition of Galectin-3 pathway prevents Isoproterenol-Induced left ventricular dysfunction and fibrosis in mice, Hypertension 67 (2016) 606–612, https://doi.org/10.1161/HYPERTENSIONAHA.115.06161.
[22] G. Vergaro, A. Del Franco, A. Carecci, Y.F. Ferrari Chen, A. Aimo, F. Forini, et al., Effects of sacubitril-valsartan on remodelling, fibrosis and mitochondria in a murine model of isoproterenol-induced left ventricular dysfunction, Aug 15, Int J. Cardiol. 409 (2024), https://doi.org/10.1016/j.ijcard.2024.132203.
[23] A. Garnier, J.K. Bendall, S. Fuchs, B. Escoubet, F. Rochais, J. Hoerter, et al., Cardiac specific increase in aldosterone production induces coronary dysfunction in aldosterone synthase-transgenic mice, Circulation 110 (2004) 1819–1825, https://doi.org/10.1161/01.CIR.0000142858.44680.27.
[24] G. Riccio, G. Esposito, E. Leoncini, R. Contu, G. Condorelli, M. Chiariello, et al., Cardiotoxic effects, or lack thereof, of anti-ErbB2 immunoagents, FASEB J. 23 (2009) 3171–3178, https://doi.org/10.1096/fj.09-131383.
[25] G. Riccio, S. Antonucci, C. Coppola, C. D'Avino, G. Piscopo, D. Fiore, et al., Ranolazine attenuates trastuzumab-induced heart dysfunction by modulating ROS production, Front Physiol. 9 (2018), https://doi.org/10.3389/fphys.2018.00038.
[26] M. Liu, J. Lv, Z. Pan, D. Wang, L. Zhao, X. Guo, Mitochondrial dysfunction in heart failure and its therapeutic implications, Front. Cardiovasc. Med. 9 (2022), https://doi.org/10.3389/fcvm.2022.945142.
[27] A. Arinno, C. Maneechote, T. Khuanjing, N. Prathumsap, T. Chunchai, B. Arunsak, et al., Melatonin and metformin ameliorated trastuzumab-induced cardiotoxicity through the modulation of mitochondrial function and dynamics without reducing its anticancer efficacy, Biochim Biophys. Acta Mol. Basis Dis. 1869 (2023), https://doi.org/10.1016/j.bbadis.2022.166618.
[28] P. Sysa-Shah, C.G. Tocchetti, M. Gupta, P.P. Rainer, X. Shen, B.H. Kang, et al., Bidirectional cross-regulation between ErbB2 and β-adrenergic signalling pathways, Cardiovasc Res 109 (2016) 358–373, https://doi.org/10.1093/cvr/cvv274.
[29] M.S. Avila, S.M. Ayub-Ferreira, M.R. de Barros Wanderley, F. das Dores Cruz, S. M. Gonçalves Brandão, V.O.C. Rigaud, et al., Carvedilol for prevention of Chemotherapy-Related cardiotoxicity: the CECCY trial, J. Am. Coll. Cardiol. 71 (2018) 2281–2290, https://doi.org/10.1016/j.jacc.2018.02.049.
[30] M. Guglin, J. Krischer, R. Tamura, A. Fink, L. Bello-Matricaria, W. McCaskill-Stevens, et al., Randomized trial of lisinopril versus carvedilol to prevent trastuzumab cardiotoxicity in patients with breast cancer, J. Am. Coll. Cardiol. 73 (2019) 2859–2868, https://doi.org/10.1016/j.jacc.2019.03.495.
[31] C. Zhang, S. He, Y. Li, F. Li, Z. Liu, J. Liu, et al., Bisoprolol protects myocardium cells against ischemia/reperfusion injury by attenuating unfolded protein response in rats, Sci. Rep. 7 (2017), https://doi.org/10.1038/s41598-017-12366-8.
[32] J. Liu, Y. Xie, Z. Han, H. Wang, W. Xu, Protective effects of bisoprolol against cadmium-induced myocardial toxicity through inhibition of oxidative stress and NF-κB signalling in rats, J. Vet. Res 65 (2021) 505–511, https://doi.org/10.2478/jvetres-2021-0054.
[33] M. Lódi, V. Bánhegyi, B. Bódi, A. Gyöngyösi, Á. Kovács, A. Árokszállási, et al., Prophylactic, single-drug cardioprotection in a comparative, experimental study of doxorubicin-induced cardiomyopathy, J. Transl. Med 18 (2020), https://doi.org/10.1186/s12967-020-02564-w.
[34] M.A. Ibrahim, O.M. Ashour, Y.F. Ibrahim, H.I. EL-Bitar, W. Gomaa, S.R. Abdel-Rahim, Angiotensin-converting enzyme inhibition and angiotensin AT1-receptor antagonism equally improve doxorubicin-induced cardiotoxicity and nephrotoxicity, Pharm. Res 60 (2009) 373–381, https://doi.org/10.1016/j.phrs.2009.05.007.
[35] A. Abareshi, F. Norouzi, F. Asgharzadeh, F. Beheshti, M. Hosseini, M. Farzadnia, et al., Effect of angiotensin-converting enzyme inhibitor on cardiac fibrosis and oxidative stress status in lipopolysaccharide-induced inflammation model in rats, Int J. Prev. Med 8 (2017), https://doi.org/10.4103/ijpvm.IJPVM_322_16.
[36] Y. Zhang, L. Zhang, X. Fan, W. Yang, B. Yu, J. Kou, et al., Captopril attenuates TAC-induced heart failure via inhibiting Wnt3a/β-catenin and Jak2/Stat3 pathways, Biomed. Pharm. 113 (2019), https://doi.org/10.1016/j.biopha.2019.108780.
[37] H. Vavřínková, M. Tutterová, P. Stopka, J. Divišová, L. Kazdová, Z. Drahota, The effect of captopril on nitric oxide formation and on generation of radical forms of mitochondrial respiratory chain compounds in ischemic rat heart, Physiol. Res 50 (2001) 481–489, https://doi.org/10.33549/physiolres.930057.
[38] M.A. Rossi, S.G. Ramos, C.M. Prado, Chronic inhibition of nitric oxide synthase induces hypertension and cardiomyocyte mitochondrial and myocardial collagen remodelling in the absence of hypertrophy, J. Hypertens. 21 (2003) 993–1001, https://doi.org/10.1097/00004872-200305000-00025.
[39] J. Mujkošová, O. Uličná, I. Waczulíková, J. Vlkovičová, O. Vančová, M. Ferko, et al., Mitochondrial function in heart and kidney of spontaneously hypertensive rats: influence of captopril treatment, Gen. Physiol. Biophys. 29 (2010) 203–207, https://doi.org/10.4149/gpb_2010_02_203.
[40] S.F. El-Sayed, A.M. Abdelhamid, S.G. ZeinElabdeen, D.I. El-Wafaey, S.M.M. Moursi, Melatonin enhances captopril mediated cardioprotective effects and improves mitochondrial dynamics in Male wistar rats with chronic heart failure, Sci. Rep. 14 (2024) 575, https://doi.org/10.1038/s41598-023-50730-z.